Type IV Cracking Susceptibility in Weld Joints of Different Grades of Cr-Mo Ferritic Steel

K. LAHA, K.S. CHANDRAVATHI, P. PARAMESWARAN, and
K. BHANU SANKARA RAO

Relative type-IV cracking susceptibility in 2.25Cr-1Mo, 9Cr-1Mo, and 9Cr-1MoVNb ferritic steel weld joint has been assessed. The type-IV cracking was manifested as preferential accumulation of creep deformation and cavitation in the relatively soft intercritical region of heat affected zone of the weld joint. The type-IV cracking susceptibility has been defined as the reduction in creep-rupture strength of weld joint compared to its base metal. The 2.25Cr-1Mo steel exhibited more susceptibility to type-IV cracking at relatively lower temperatures; whereas, at higher temperatures, 9Cr-1MoVNb steel was more susceptible. The relative susceptibility to type-IV cracking in the weld joint of the Cr-Mo steels has been rationalized on the basis of creep-strengthening mechanisms operating in the steels and their venerability to change on intercritical heating during weld thermal cycle, subsequent postweld heat treatment, and creep exposure.

DOI: 10.1007/s11661-008-9724-x

I. INTRODUCTION

THE Cr-Mo ferritic steels are widely used in fabrication of power plants and petrochemical industries. Different grades of Cr-Mo ferritic steel with chromium in the range 0.5 to 12.0 wt pct and Mo in the range 0.25 to 2.0 wt pct are in use, and the selection of a specific grade is based on their creep-rupture strength and oxidation resistance. The Cr-Mo ferritic steels derive their creep strength from the solid-solution strengthening, precipitation strengthening by the complex inter- and intragranular metal carbonitride particles and from the phase-transformation induced dislocation substructures. The strengthening mechanisms are vulnerable to change on thermal and creep exposures, and degradation in creep strength of the steels occurs on service exposure. Large-scale plants are usually fabricated employing fusion-welding techniques. The deposited weld metal and the heat affected zone (HAZ) of the base metal of the joint have different microstructures possessing appreciably different mechanical properties than the base metal.[1,2] These result in creep-rupture strength of Cr-Mo ferritic steel weld joint lower than the base metal due to the different types of cracking developed during creep exposure.[3] Type-IV cracking at the outer range of HAZ is considered life-limiting factor of high-temperature welded components fabricated out of Cr-Mo ferritic steels.[4]

To decrease environmental pollution by CO_2 emission, the traditionally used 2.25Cr-1Mo steel is now increasingly replaced by higher creep-resistant 9Cr-1MoVNb (modified 9Cr-1Mo) steel in an effort to increase the efficiency of power plants by operating them at higher temperatures and pressures. However, many concerns have been reported regarding the premature failure of welded components fabricated out of the more advanced higher creep-resistant ferritic steels.[5,6] This study is concerned with the relative susceptibility to type-IV cracking under creep condition in the weld joint of different grades of Cr-Mo steel. The steels investigated are low-chromium 2.25Cr-1Mo (grade 22) and high-chromium 9Cr-1Mo (grade 9), and 9Cr-1MoVNb (grade 91).

II. EXPERIMENTAL DETAILS

The chemical compositions of the 2.25Cr-1Mo, 9Cr-1Mo, and 9Cr-1MoVNb steels are shown in Table I. The steels were received in normalized and tempered conditions. The normalization was carried out at 1223 K for 17 minutes, 1223 K for 15 minutes, and 1333 K for 6 hours; whereas, tempering was carried out at 1003 K for 1 hours, 1053 K for 2 hours, and 1043 K for 4 hours, respectively, for the 2.25Cr-1Mo, 9Cr-1Mo, and 9Cr-1MoVNb steels. Similar weld joints of the steels were fabricated by a manual metal arc welding process employing a basic coated respective matching weld electrode. The chemical compositions of the deposited weld metals are also shown in Table I. The weld pads of the 2.25Cr-1Mo, 9Cr-1Mo, and 9Cr-1MoVNb steels were subjected to a postweld heat treatment (PWHT) for 1 hour at 973, 1023, and 1033 K, respectively, and were subsequently X-ray radiographed for their soundness. Optical metallography, transmission electron

K. LAHA, Scientific Officer "G", K.S. CHANDRAVATHI, Scientific Officer "E", P. PARAMESWARAN, Scientific Officer "F", and K. BHANU SANKARA RAO, Associate Director, Materials Development and Characterization, are with the Metallurgy and Materials Group, Indira Gandhi Center for Atomic Research, Kalpakkam 603 102, India. Contact e-mail: laha@igcar.gov.in
Manuscript submitted on July 30, 2007.
Article published online December 20, 2008

Table I. Chemical Compositions of the Steels and the Deposited Weld Metals (Weight Percent)

Material	C	Si	Mn	P	S	Cr	Mo	Ni	V	Nb	N	Fe
2.25Cr-1Mo Base metal	0.06	0.18	0.47	0.008	0.008	2.18	0.93	—	—	—	—	bal
2.25Cr-1Mo Weld metal	0.05	0.40	0.72	0.02	0.012	2.30	1.10	—	—	—	—	bal
9Cr-1Mo Base metal	0.10	0.49	0.46	0.008	0.002	8.36	0.93	—	—	—	—	bal
9Cr-1Mo Weld metal	0.12	0.52	0.52	0.003	0.03	8.90	0.98	—	—	—	—	bal
9Cr-1MoVNb Base metal	0.096	0.32	0.46	0.01	0.008	8.72	0.90	0.10	0.22	0.08	0.05	bal
9Cr-1MoVNb Weld metal	0.098	0.35	0.58	0.011	0.008	8.63	1.02	0.63	0.20	0.06	0.06	bal

microscopy (TEM), and microhardness testing were carried out across the joint of the steels.

To simulate HAZ microstructures, the base steels were subjected to heat treatments consisting of soaking for 5 minutes at temperatures in the range 973 K to 1333 K (below Ac_1 to above Ac_3), followed by oil quenching and subsequent tempering at respective PWHT conditions. The simulation of HAZ was based on the detailed comparison of the prior austenitic grain size, hardness, and the microconstituents of the 5-minute soaking heat-treated samples of the steel with those of the actual HAZ of the steel weld joints.[7] Hardness, tensile, and creep tests were carried out on the heat-treated steels.

Creep tests were carried out on the steels and their weld joints over a stress range of 50 to 275 MPa at 773 K, 823 K, and 873 K. Creep specimens were of 5-mm diameter and 50-mm length. Creep-deformation inhomogeneity across the weld-joint specimen was monitored by interrupting specially conducted creep tests at periodic intervals and measuring the distance between the hardness-indentation marks made across the weld-joint specimen before creep test. Creep-ruptured joint specimens were sectioned longitudinally and mechanically polished to carry out the microhardness testing and scanning electron microscopy (SEM). A series of SEM photographs were taken of the creep-exposed weld joints of the steels. The photographs were analyzed to estimate the accumulated creep cavitation across the different constituents of the steel weld joints. Transmission electron microscopy was carried out on creep-exposed joints of the steels.

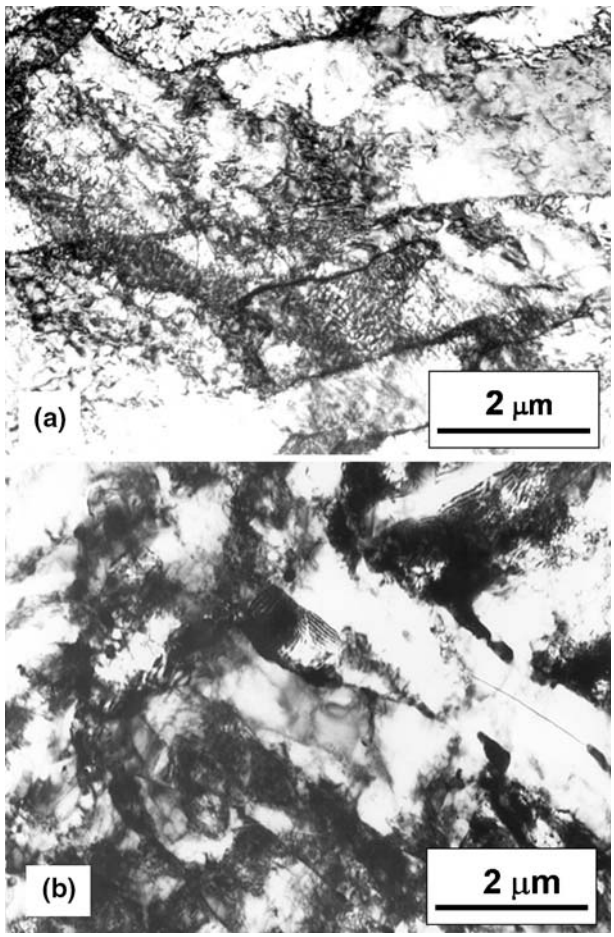

Fig. 1—TEM micrographs of the steels (*a*) 2.25Cr-1Mo and (*b*) 9Cr-1MoVNb.

III. RESULTS AND DISCUSSION

A. *Soft-Zone Formation in Weld Joint of Cr-Mo Steels*

Microstructure across the Cr-Mo steel weld joint was found to vary in a complicated manner. The 2.25Cr-1Mo base metal (Figure 1(a)) and weld metal had bainitic structure, and the HAZ was comprised of coarse prior-austenitic grain bainite, fine prior-austenitic grain bainite, an intercritically heated (between Ac_1 and Ac_3) two-phase region, and an over-tempered (below Ac_1) zone, in an order away from the weld-fusion interface toward the unaffected base metal.[7] Both the 9Cr steel (9Cr-1Mo and 9Cr-1MoVNb) base metals (Figure 1(b)) and weld metals had martensite structures and the HAZ consisted of coarse prior-austenitic grain martensite, fine prior-austenitic grain martensite, intercritical, and over-tempered regions.[8,9] The hardness across the joints of the steels varied significantly (Figure 2). A relatively soft zone was observed at the outer edge of the HAZ of the steels weld joints. The hardness variation across the weld joint was found less in the 9Cr-1Mo steel than that in the 2.25Cr-1Mo and 9Cr-1MoVNb steels (Figure 2).

The microstructures developed across the HAZ and the location of soft zone in it can be rationalized on the basis of the peak temperatures experienced by the base metal during weld thermal cycle and the phase-transformation characteristic of the steel.[2,7–9] The region of the HAZ closest to the weld-fusion boundary experiences peak temperature well above the $[(\alpha + \gamma)/\gamma]$ (Ac_3) phase transformation. At these temperatures, the carbides that impede the austenite grain growth dissolved, resulting in the formation of coarse-austenite grain. On cooling, the coarse-grain austenite transforms into

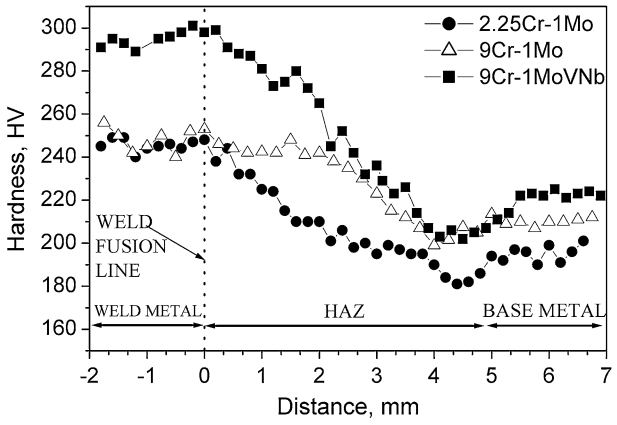

Fig. 2—Microhardness variation across the weld joints of 2.25Cr-1Mo, 9Cr-1Mo, and 9Cr-1MoVNb steels.

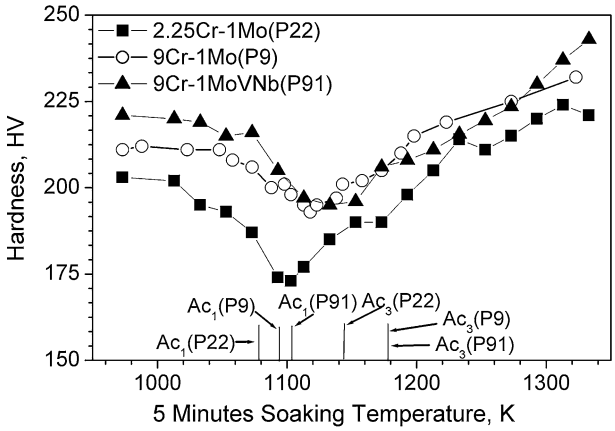

Fig. 3—Variation of hardness with 5-min soaking at temperatures in the range below the Ac_1 to above the Ac_3 of the 2.25Cr-1Mo, 9Cr-1Mo, and 9Cr-1MoVNb steels (in tempered condition).

bainite in 2.25Cr-1Mo steel and martensite in both the 9Cr steels. The prior-austenitic grain size decreases with increasing distance from the weld-fusion line as the peak temperature experienced decreases. The HAZ that experiences peak temperatures just above the transformation temperature Ac_3 possesses very fine (approximately 10 μm) prior-austenitic grain. When the thermal-cycle peak temperature experienced is in the range between the Ac_1 [$\alpha/(\alpha + \gamma)$] and Ac_3 (intercritical range), only partial transformation to austenite could occur during heating of the weld thermal cycle. The intercritical microstructures resulting on subsequent cooling would be a mixture of two phases: one being the freshly formed austenite-transformation product (bainite/martensite), and the other being the untransformed ferrite (initial tempered bainite/martensite).[7] Below Ac_1, the steels merely are tempered.

Intercritical heating of the steels followed by quenching resulted in higher hardness than on subcritical heating (below Ac_1).[7,8] The portion of the ferrite that had been re-austenitized on intercritical heating transformed into bainite/martensite on quenching to have high hardness. The untransformed ferrite merely tempered extensively. The temperatures in the intercritical range are not expected to dissolve the pre-existing carbides appreciably. The carbides could be either coarsened by Ostwald-ripening mechanism; whereby, the relatively coarser particles increase in size at the expense of the relatively fine particles or the existing carbides are replaced by higher-order particles. Thus, the austenite formed on the intercritical heating had lower carbon content in solution than that expected from the usual normalization when the majority of the prior-existing carbides dissolve. The low-carbon austenite transformed on subsequent cooling into bainite/martensite. On subsequent tempering at temperatures below Ac_1, no further secondary precipitation is expected in the heavily tempered ferrite and much less secondary precipitation is expected in the bainite/martensite derived from the low-carbon austenite. The microstructural features described above led to an enhanced recovery in the intercritical structure compared to the other regions of the HAZ on subsequent tempering to form a soft zone in weld joint (Figure 2). The variations of hardness of the Cr-Mo steels with a 5-minute soaking temperature followed by tempering show lower hardness on intercritical soaking (Figure 3). The exercise of heating the base steels has proved quite unambiguously that the soft-zone formation in the weld joint of these steels (Figure 2) was in the intercritical region of the HAZ adjacent to the overtempered HAZ and the unaffected base metal.

B. *Creep-Strength Heterogeneity across Cr-Mo Steel Weld Joint*

The variations of creep-rupture life with applied stress at 823 K of the 2.25Cr-1Mo, 9Cr-1Mo, and 9Cr-1MoVNb steels and their weld joints are shown in Figure 4. The 9Cr-1MoVNb steel possessed higher creep-rupture strength than both the 2.25Cr-1Mo and 9Cr-1Mo steels. The 2.25Cr-1Mo and 9Cr-1Mo steels

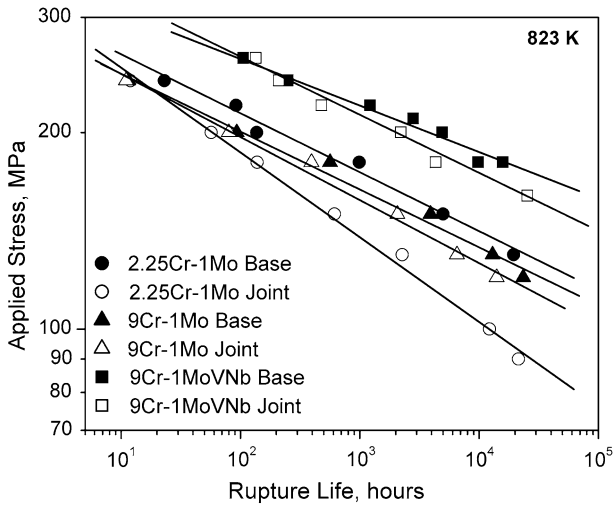

Fig. 4—Variation of creep-rupture life with applied stress for the 2.25Cr-1Mo, 9Cr-1Mo, and 9Cr-1MoVNb steel-base metals and their weld joints at 823 K.

had comparable creep-rupture strength. The weld joints of the steels had lower creep-rupture strength than their respective base metals. Creep-rupture strength of the 2.25Cr-1Mo and 9Cr-1MoVNb steels and their weld joints at different temperatures are displayed as Larson–Miller parameter, $P = T(C + \log t_r)$ in Figures 5(a) and (b), respectively.[10,11] The difference in creep-rupture strength between the base metal and weld joint increased with an increase in creep-rupture life and testing temperature, and the difference was found to depend on the grade of the Cr-Mo steel. At 823 K, the difference was higher for the 2.25Cr-1Mo steel and lower for the 9Cr-1Mo steel (Figure 4). Macrostructure of the failed joint specimen (Figure 6) reveals that the failure occurred in the HAZ close to the base metal, commonly known as type-IV failure.[3]

The variation of steady-state creep rate with applied stress of the different constituents of the 2.25Cr-1Mo weld joint (*viz*. base metal, weld metal, coarse-grain HAZ, fine-grain HAZ, and intercritical HAZ) is compared in Figure 7, showing high creep-strength heterogeneity among the constituents of the weld joint.

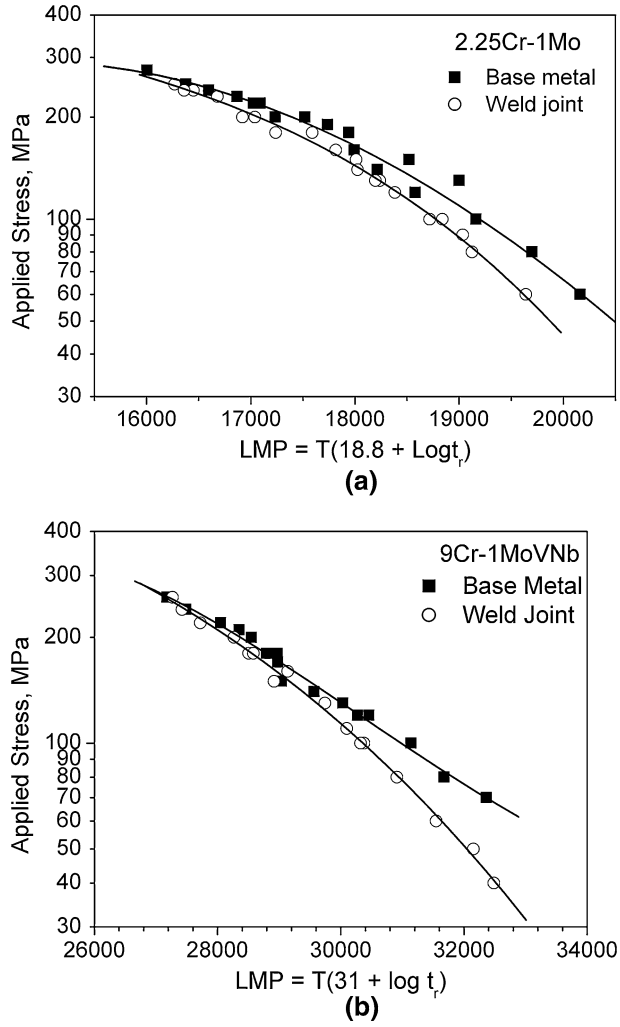

Fig. 5—Larson–Miller plots for rupture lives of the steels and their weld joint of (*a*) 2.25Cr-1Mo and (*b*) 9Cr-1MoVNb steels.

The coarse-grain bainitic HAZ possessed the lowest creep rate; whereas, the intercritical HAZ had the highest. Similar variations in creep properties among the different constituents of the 9Cr steel weld joint have been reported.[1] The existing strength heterogeneity across the weld joint of the Cr-Mo steels is expected to yield complex deformation behavior of weld joint especially under creep condition. Finite-element analysis of the equivalent creep strain and the principal stress across the 2.25Cr-1Mo steel weld joint was carried out employing the creep-deformation properties of the different constituents of the joint. Figure 8 shows the variations of creep strain and principal stress across the 2.25Cr-1Mo steel weld joint creep tested at 823 K and 150 MPa for 500 hours, in both the central and surface locations of the creep specimen. The analysis predicts a preferential creep deformation in the soft intercritical region of HAZ. The experimental-measured accumulation of creep deformation across the different constituents of the 2.25Cr-1Mo and 9Cr-1Mo steels weld joint during creep test at 150 MPa and 823 K are compared in Figure 9. As predicted by finite-element analysis (Figure 8), a pronounced localization of creep deformation in the soft intercritical/fine-grain region of HAZ in the steels weld joint was observed, which ultimately led to failure of the joints in this zone (Figure 6). A similar creep-strain concentration in the soft intercritical region of HAZ was predicted and validated in modified 9Cr-1Mo steel welded pipe by Eggeler *et al*.[18] It is to be noted that the creep-straining inhomogeneity was more pronounced in the 2.25Cr-1Mo steel weld joint

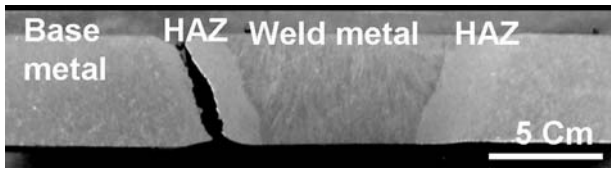

Fig. 6—Location of creep failure in the 9Cr-1MoVNb steel weld joint.

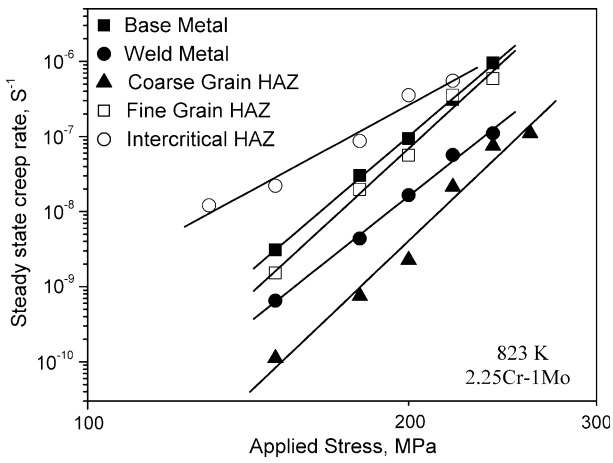

Fig. 7—Variation of steady-state creep rate with applied stress of the different constituents of 2.25Cr-1Mo steel weld joint at 823 K.

than that in the 9Cr-1Mo steel weld joint (Figure 9), and this, as discussed later, has a strong implication on the type-IV cracking susceptibility of different Cr-Mo steels.

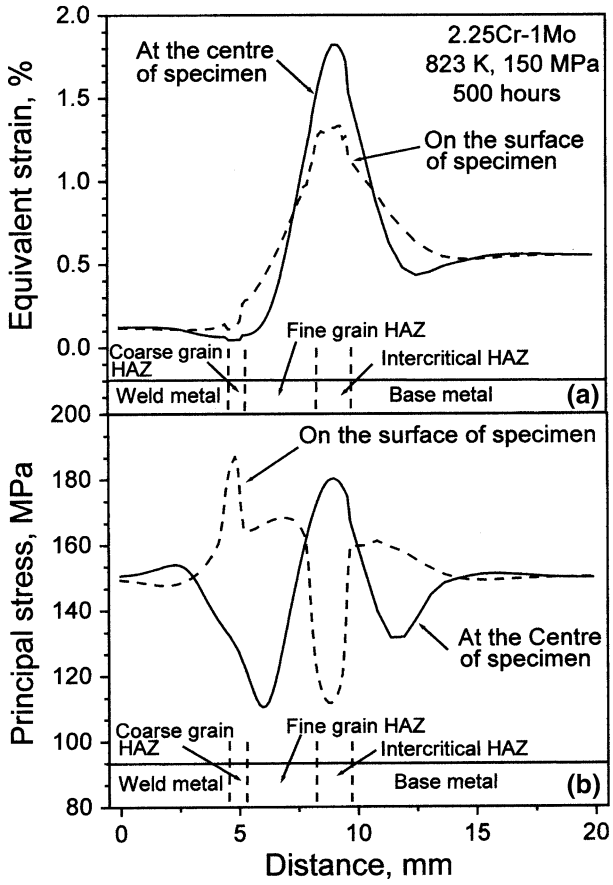

Fig. 8—Finite-element analysis of creep strain and principal stress across the weld joint of 2.25Cr-1Mo steel creep tested at 150 MPa and 823 K for 500 h.

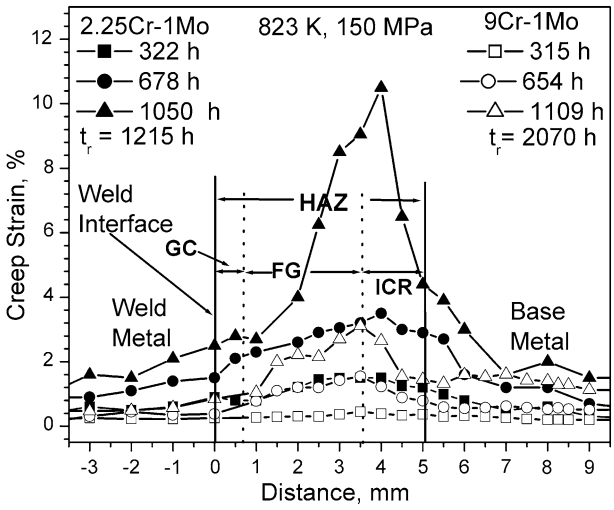

Fig. 9—Progress in creep deformation at 823 K and 150 MPa across the weld joint of the 2.25Cr-1Mo and 9Cr-1Mo steels.

C. *Characteristic of Type-IV Cracking*

Macrostructure of the 9Cr-1MoVNb steel weld joint creep tested at 823 K and 160 MPa (t_r = 25,422 hours) containing the type-IV crack is shown in Figure 10. Type-IV cracks developed in the central location of intercritical region of HAZ in the weld joint. Similar type-IV cracks were observed in the weld joints of the other two Cr-Mo steels. Coalescence of creep cavities led to the type-IV cracking. The cracking started at the central region of the creep specimen and propagated outward to the surface by coalescence of creep cavities ahead of the crack. The creep cavitation was predominantly confined to the intercritical region of HAZ (Figure 11), which experienced more pronounced localized creep deformation (Figures 8 and 9)[12,13] leading to type-IV failure in the intercritical region of HAZ. A triaxial state of stress developed across the weld joint during creep test because of the creep-strength inhomogeneity across it (Figure 8) and has been reported by many investigators.[14,15] The highly localized stress region in the center of the specimen (Figure 8) promoted creep cavitation at the interior region of intercritical HAZ (Figure 10), because the creep cavitation is predominately controlled by the principal stress.[16] Interrupted creep test revealed that the creep cavities are associated with coarse-precipitate particles in the intercritical region of HAZ (Figure 12).[12,13]

Scanning electron microscopy fractographs of the simulated intercritical HAZ of the 2.25Cr-1Mo steel and

Fig. 10—Macrocrack at HAZ in 9Cr-1MoVNb steel weld joint (creep tested at 823 K, 160 MPa, and t_r = 25,422 h).

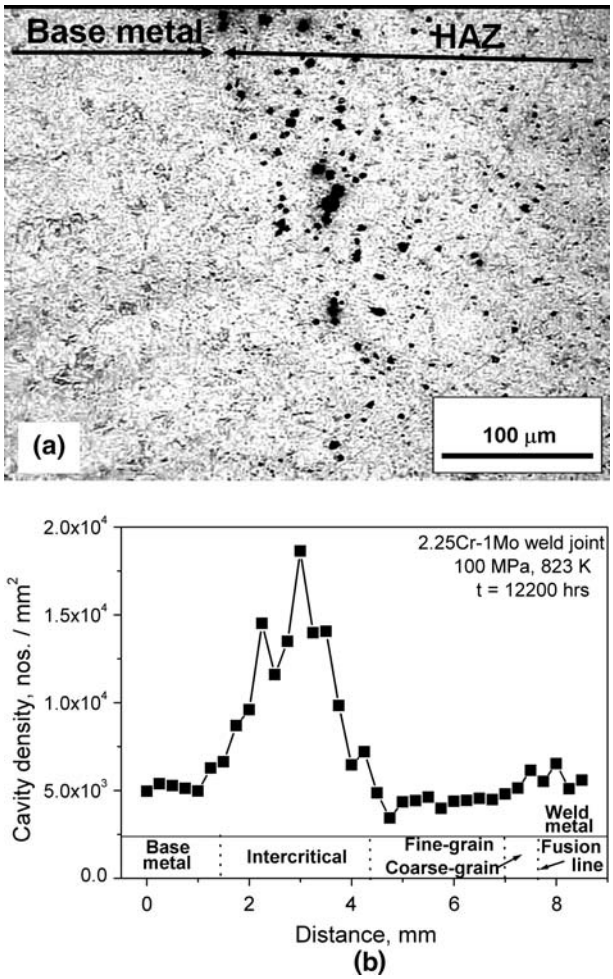

Fig. 11—(*a*) Preferential creep cavitation in the intercritical region of HAZ in 9Cr-1MoVNb steel weld joint (923 K, 40 MPa, and t_r = 15,721 h, and (*b*) creep-cavity density (nos/mm^3) across creep fractured (873 K, 100 MPa, and t_r = 12,200 h) weld joint of 2.25Cr-1Mo steel.

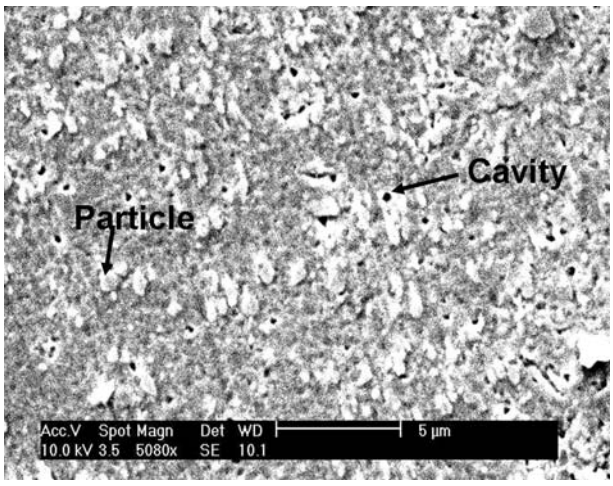

Fig. 12—SEM micrograph of interrupted creep tested (40 MPa, 923 K for 9881 h, and t/t_r = 0.64) 9Cr-1MoVNb steel weld joint, showing type-IV creep-cavity nucleation associated with the coarse particles in the intercritical HAZ.

its weld joint failed in the intercritical region of HAZ under creep conditions are shown in Figure 13. Typical transgranular dimple failure was observed in the simulated intercritical HAZ (Figure 13(a)). Mixed mode failure comprising transgranular dimple and intergranular creep cavities was observed in the weld joint which

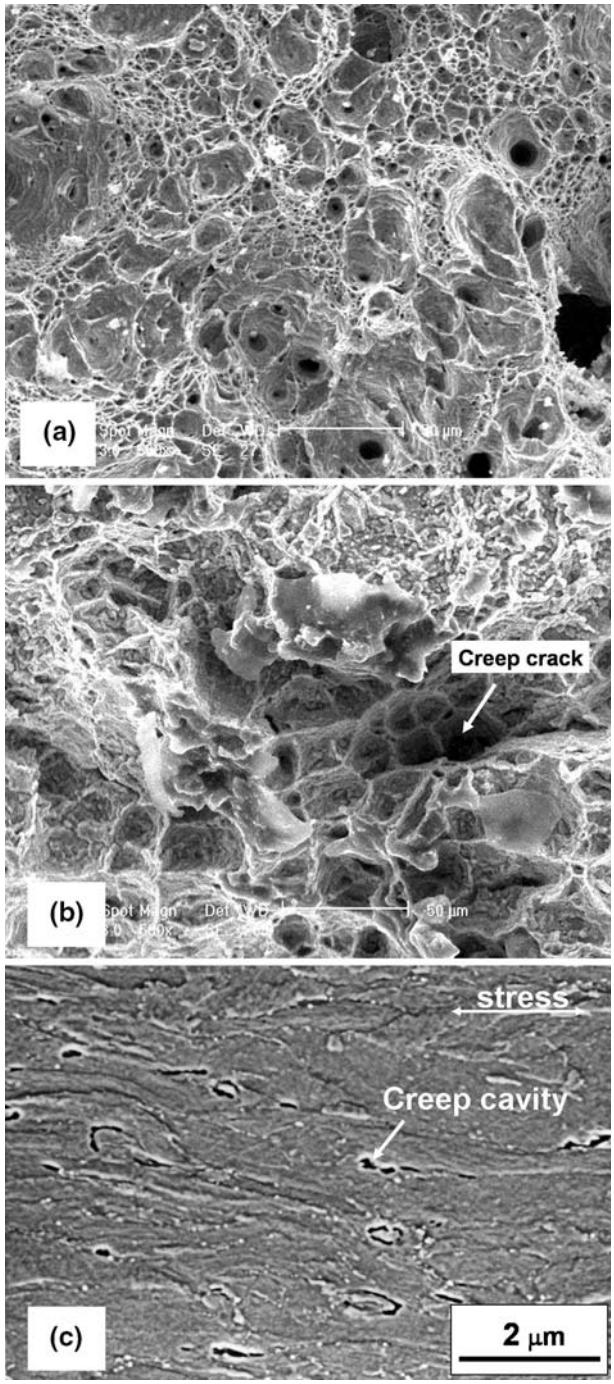

Fig. 13—SEM micrographs (*a*) ductile dimple fracture in simulated intercritical HAZ of 2.25Cr-1Mo steel (130 MPa, 823 K, and t_r = 1456 h), (*b*) mixed-mode dimple and intergranular creep failure in 2.25Cr-1Mo weld joint (150 MPa, 823 K, and t_r = 1267 h), and (*c*) creep cavitation along with creep strain in intercritical HAZ of 2.25Cr-1Mo steel weld joint (150 MPa, 823 K, and t_r = 1267 h).

failed in the intercritical HAZ (Figure 13(b)). The localized creep deformation and intergranular creep cavitation in type-IV cracking (Figure 13(c)) led to mixed-mode creep failure as illustrated by intergranular creep cracks surrounded by intragranular dimples in the weld joint (Figure 13(b)). At higher temperatures, more predominant intergranular creep cavitation was observed in the 9Cr-1MoVNb steel weld joint than in the 2.25Cr-1Mo steel weld joint. Fine-grain size may also promote creep cavitation in the intercritical HAZ. However, the transgranular dimple failure of the simulated intercritical HAZ (Figure 13(a)) reveals that fine-grain size of intercritical HAZ might not be the main reason for the localized creep cavitation in the joint. The triaxial state of stress resulted from the "metallurgical notch" induced creep cavitation in the soft intercritical region of HAZ in the Cr-Mo ferritic steels weld joint to produce type-IV failure.

D. *Relative Type-IV Cracking Susceptibility of Cr-Mo Steels*

The reduction in creep-rupture strength of weld joint depends on the type of the Cr-Mo steel (Figures 4 and 5). The type-IV cracking susceptibility has been defined as a percentage reduction in creep-rupture strength of the steel weld joint compared to its base metal for a specific creep-rupture life. The percentage reduction in creep-rupture strength of the weld joint of the steels at 823 K is compared in Figure 14. The 2.25Cr-1Mo steel was found more susceptible to type-IV cracking than the 9Cr-1MoVNb steel, and the 9Cr-1Mo was least susceptible. The percentage reductions in creep-rupture strength of the weld joint at different temperatures are plotted as a function of rupture life for the 9Cr-1MoVNb and 2.25Cr-1Mo steels in Figures 15(a) and (b), respectively. The temperature sensitivity of the susceptibility to type-IV cracking in the steels weld joint (strength reduction) was found to be more in the 9Cr-1MoVNb steel than that in the 2.25Cr-1Mo steel. At higher test temperature, the 9Cr-1MoVNb steel was found more susceptible to type-IV cracking than the 2.25Cr-1Mo steel.

The type-IV cracking occurs in the intercritical region of HAZ (Figure 11). The reduction in creep-rupture strength of Cr-Mo steel weld joint due to type-IV cracking and the different susceptibility to type-IV cracking of the steels can be rationalized on the basis of creep-strengthening mechanisms operating in the steels and their modification on intercritical heating during weld thermal cycle and, subsequently, on thermal and creep exposures.

1. *Strengthening mechanism in Cr-Mo steels*

The Cr-Mo ferritic steels derive their creep strength from solid-solution strengthening, dislocation-substructure strengthening, and precipitation strengthening.[17,18] Molybdenum promotes solid-solution strengthening of the Cr-Mo steels. The 2.25Cr-1Mo steel on normalization undergoes transformation to bainitic structure (Figure 1(a)) and the 9Cr steel to martensitic structure

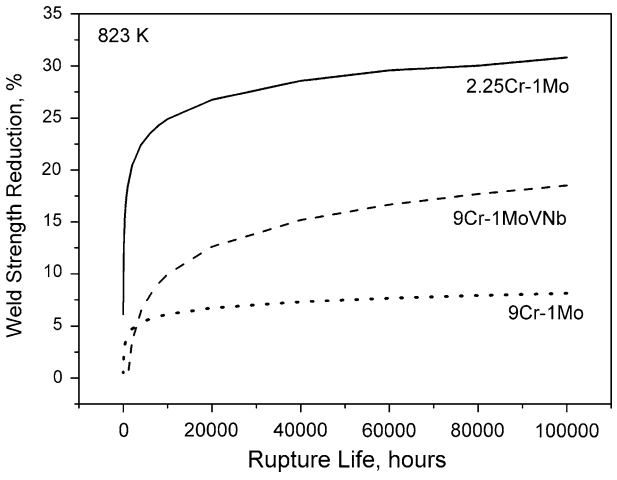

Fig. 14—Variation of the weld creep-strength reduction percentage of the steels with rupture life at 823 K.

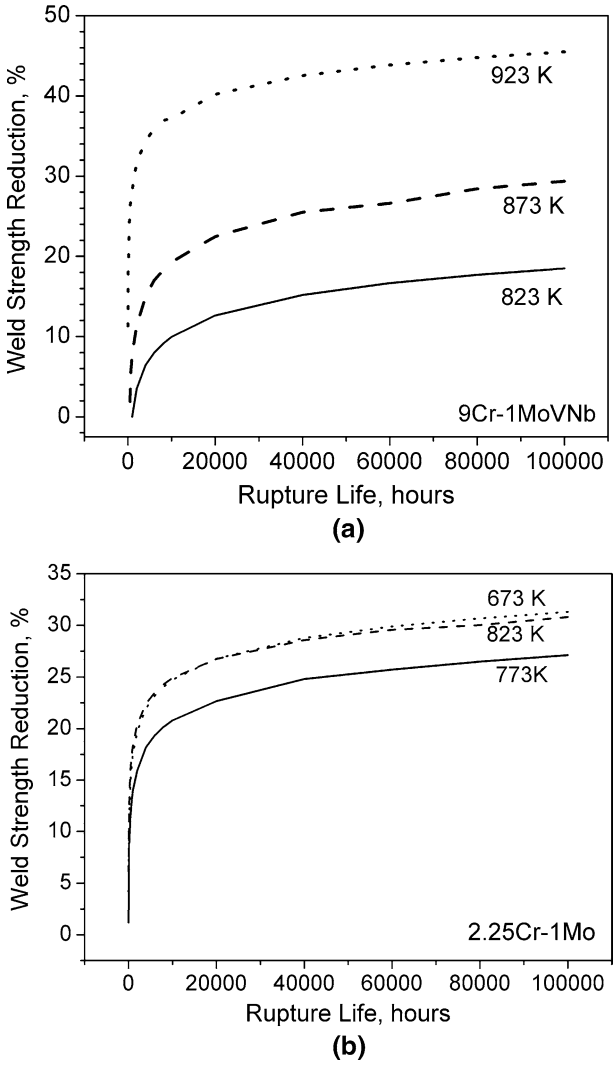

Fig. 15—Variation of the weld creep-strength reduction percentage of the steels (*a*) 9Cr-1MoVNb and (*b*) 2.25Cr-1Mo with rupture life at different test temperatures.

(Figure 1(b)). On tempering, the bainitic/martensitic lath structures change to subgrain structures by the lateral fragmentation of laths but still retain a high-dislocation density. A relatively coarser dislocation subgrain structure develops on tempering in the bainitic 2.25Cr-1Mo steel than in the martensitic 9Cr steels (Figure 1).

Tempering of the Cr-Mo steels subsequent to normalization promotes the precipitation of various types of carbonitride particles. The general sequence of the precipitation of carbides in 2.25Cr-1Mo steel on tempering has been reported by Baker and Nutting.[19] The most effective creep strengthening in 2.25Cr-1Mo steel results from the fine dispersions of semicoherent acicular Mo_2C particles. However, the Mo_2C precipitates are relatively less stable against thermal and creep exposures and are eventually replaced by molybdenum-rich M_6C through the intermediate precipitation of M_7C_3 (chromium and molybdenum rich) and $M_{23}C_6$ (chromium rich).[19] The normalized martensitic 9Cr-1Mo steel contains autotempered Fe-rich M_3C type of carbides.[17] During tempering, Cr-rich $M_{23}C_6$ carbides precipitate at grain and subgrain boundaries as coarse particles and serve as agents for stabilizing the subgrain structures and, thus, indirectly contribute to the creep strengthening. In 9Cr-1MoVNb steel, the additions of V, Nb, and N ensure intragranular precipitation of highly stable V,Nb-carbonitrides (MX) particles on tempering and during creep exposure[20] to confer relatively high creep strength (Figure 4). The primary (prior existing particles retained on normalization) NbX particles act as nucleating centers for $M_{23}C_6$ precipitates and, thus, promote the precipitation of much finer and higher density of $M_{23}C_6$ precipitate in the 9Cr-1MoVNb steel than in the 9Cr-1Mo steel. Also, V can enter in the $M_{23}C_6$ to increase its coarsening resistance against thermal and creep exposures so that the $M_{23}C_6$ precipitates can stabilize the subgrain structure in 9Cr-1MoVNb steel more effectively for longer creep duration than in the 9Cr-1Mo steel. Laves phase (Fe_2M), an intermetallic compound, is found to precipitate on grain and subgrain boundaries on thermal and creep exposures in the Mo and W containing high-chromium ferritic steels. The precipitation of laves phases is expected to decrease the solid-solution strengthening but increases the precipitation strengthening of the steels, at least when they are fine in size.[21] On long-term high-temperature thermal and creep exposures, modified *Z* phase, a complex Cr(V,Nb)N particle, is reported to precipitate intergranularly in the 9Cr-1MoVNb steel.[21,22] They are fine in size just after precipitation but grow quickly by dissolving the beneficial MX types of precipitates to accelerate the recovery process of the steel to decrease its strength drastically on long-term thermal and creep exposures.

The variation in hardness of the Cr-Mo steels on thermal and creep exposures at 823 K is shown in Figure 16. The hardness of the steels decreased more significantly on creep exposure as compared to thermal exposure. The combined effect of stress and temperature in decreasing the dislocation density, coarsening the precipitates, and increasing the subgrain size have been suggested to be responsible for the more pronounced

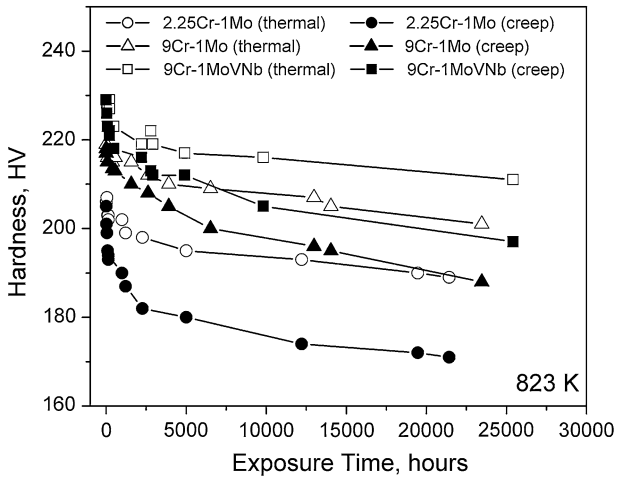

Fig. 16—Variation of the hardness of the steels on thermal and creep exposures at 823 K.

degradation in strength of the Cr-Mo steels under creep conditions.[23] The decrease in hardness with creep exposure was comparatively more in the 2.25Cr-1Mo steel and less in the 9Cr-1Mo steel. This indicates that the strengthening mechanisms operating in the 2.2Cr-1Mo steel are more prone to change on thermal and creep exposures than those in the 9Cr steels.

2. *Microstructure and type-IV cracking susceptibility*

Type-IV cracking occurred in the intercritical region of HAZ. Transmission electron microscopy micrographs of the 2.25Cr-1Mo base metal and the intercritical region of HAZ of the 2.25Cr-1Mo and the 9Cr-1MoVNb steel weld joints are shown in Figure 17. Dissolution and coarsening of the precipitates, as well as the reduction of dislocation density, were noticed in the 2.25Cr-1Mo steel upon intercritical heating during weld thermal cycle (Figure 17(a) and (b)). An almost complete absence of Mo_2C in the intercritical region of HAZ in 2.25Cr-1Mo steel weld joint had been reported by Roy and Lauritzen,[24] leading to the decrease in hardness (Figure 2). Energy dispersive X-ray spectrum (EDXS) analysis of the precipitate particles in 2.25Cr-1Mo base metal and intercritical HAZ was carried out (Figure 18). The abundantly present needle-shaped particles in the 2.25Cr-1Mo base metal (Figure 17(a)) were molybdenum-rich Mo_2C particles (Figure 18(a)). In the intercritical HAZ, a relatively smaller number of Mo_2C particles was seen (Figure 17(b)), and the relatively coarser particles were identified as chromium-rich $M_{23}C_6$ (Figure 18(b)) and molybdenum- and chromium-rich M_6C Figure 18(c)). Replacement of lathlike martensitic structure with high dislocation density in the base metal by large subgrain with low dislocation density and coarsening grain boundary and subgrain boundary carbides are evident due to intercritical heating in the 9Cr steels (Figures 1(b) and 17(c)). Lower carbide density in the intercritical region of HAZ has been reported by Laha *et al.*[12] and Li *et al.*[13] in 9Cr steels. In the 9Cr-1MoVNb steel weld joint, reduction of hardness in the intercritical region of HAZ is reported to

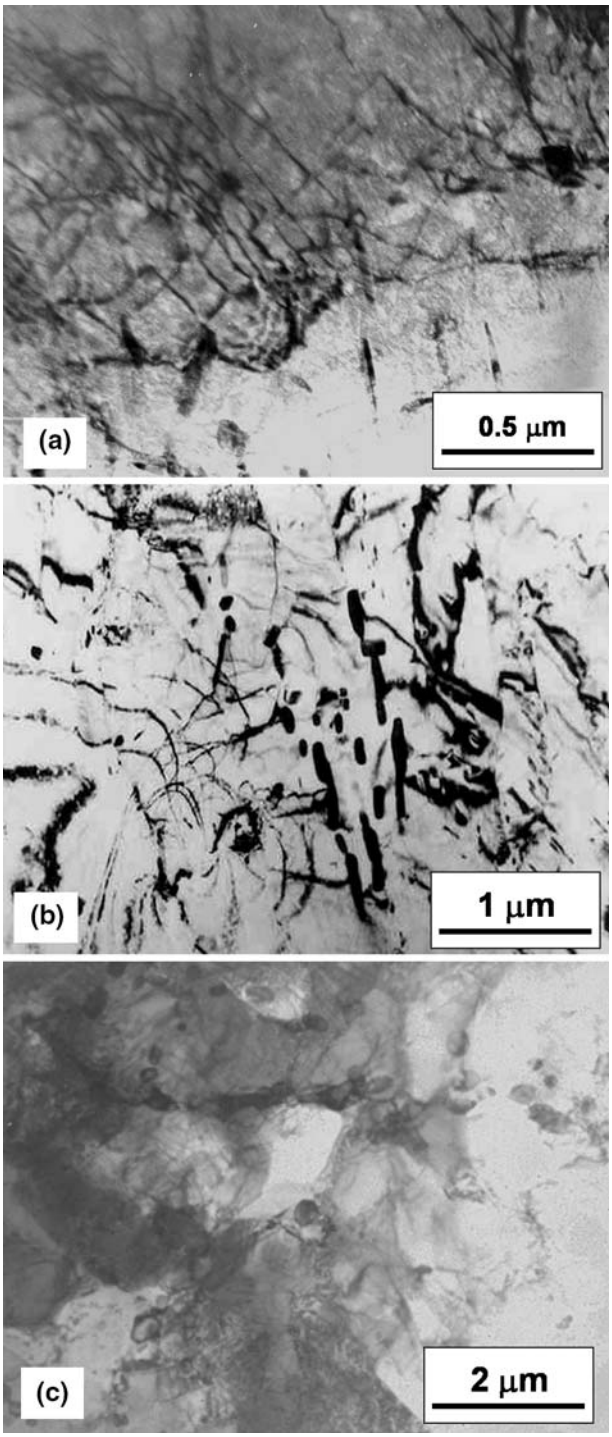

Fig. 17—TEM micrographs (*a*) 2.25Cr-1Mo base metal, (*b*) the intercritical HAZ of the weld joint of 2.25Cr-1Mo steel, and (*c*) the intercritical HAZ of the weld joint of 9Cr-1MoVNb steel.

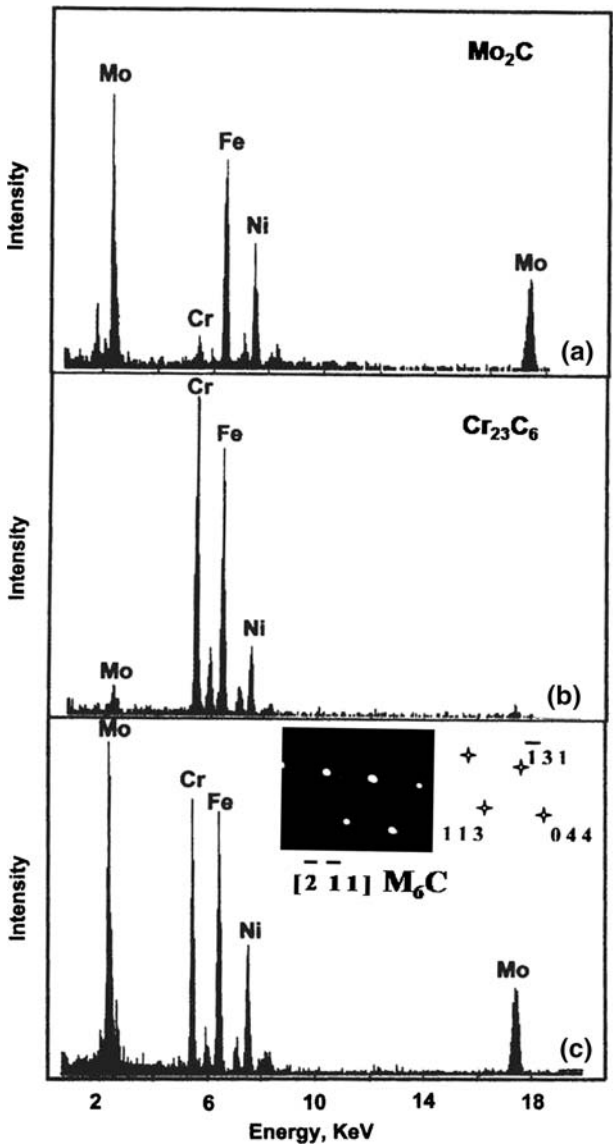

Fig. 18—EDXS of (*a*) precipitate in 2.25Cr-1Mo base metal and (*b*) and (*c*) precipitates of intercritical HAZ of 2.25Cr-1Mo steel weld joint. (Nickel peaks are from nickel grid used to hold the specimen).

be due to (1) the replacement of martensite laths with high dislocation density by large subgrains having low dislocation density, (2) the coarsening of $M_{23}C_6$ type of carbides at grain and subgrain boundaries, and (3) the change in shape of the V/Nb carbonitride particles from needle to spherical and the reduction of their misfit with matrix.[25]

The 2.25Cr-1Mo steel owes its creep strength mostly to the intragranular precipitation of Mo_2C particles. The partial/complete absence of Mo_2C in the intercritical region of HAZ (Figures 17(a) and (b)) reduced the creep strength of the 2.25Cr-1Mo steel weld joint quite extensively compared to those in the 9Cr-1Mo and 9Cr-1MoVNb steels (Figure 14). In the 9Cr steels, especially in the 9Cr-1Mo steel, the hardness reduction on intercritical heating was much less than that in the 2.25Cr-1Mo steel (Figure 3). The strengthening mechanisms operating in the 9Cr steels appear to be much less affected by the intercritical heating than those in the 2.25Cr-1Mo steel. The pronounce strength inhomogeneity across the 2.25Cr-1Mo weld joint than that in the 9Cr-1Mo steel is also reflected in the higher creep deformation rate variation across the 2.25Cr-1Mo steel weld joint during creep test (Figure 9). The dominant

occurrence of type-IV cracking in the 2.25Cr-1Mo steel reduces the creep-rupture strength of the 2.25Cr-1Mo steel joint more drastically than that of the 9Cr-1Mo steel in spite of their comparable creep-rupture strength (Figure 4).

The 2.25Cr-1Mo steel was found to be more susceptible to type IV cracking at lower test temperatures but at higher test temperatures the 9Cr-1MoNbV steel had a higher susceptibility to type IV cracking than the other two Cr-Mo steels (Figure 15). It is probable that in the 2.25Cr-1Mo steel, in the absence of Mo_2C in the intercritical region of HAZ, the higher creep-testing temperature could not further reduce the strength appreciably. In the 9Cr-1MoVNb steel, appreciable coarsening of the Cr-rich $M_{23}C_6$ carbides was observed on creep exposure, especially at higher temperatures.[21,23] The coarsening of carbides led to the enhanced recovery of the dislocation substructures. The *Z* phase was observed in the intercritical region of HAZ in 9Cr-1MoVNb steel weld joint on creep exposure (Figure 19); whereas, very little was observed in base steel. Formations of modified *Z* phase in modified 9Cr-1Mo steel on creep and thermal exposures have been reported by Danielsen and Hald.[22] It is probable that the creep-strain concentration induced more extensive precipitation of Z phase in the intercritical region of HAZ than in the base metal. The *Z*-phase precipitation is accompanied with dissolution of MX type of carbonitrides, which provide creep strength in the steel. The enhanced coarsening of the $M_{23}C_6$ particles and the precipitation of the *Z*-phase in the intercritical region of HAZ at higher creep test temperatures than that in the base metal could be the reasons for the higher reduction in creep rupture strength of the 9Cr-1MoVNb steel weld joint. These lead to the higher susceptibility to type IV cracking in 9Cr-1MoNbV steel at higher testing temperatures than in the other Cr-Mo steels investigated (Figure 15).

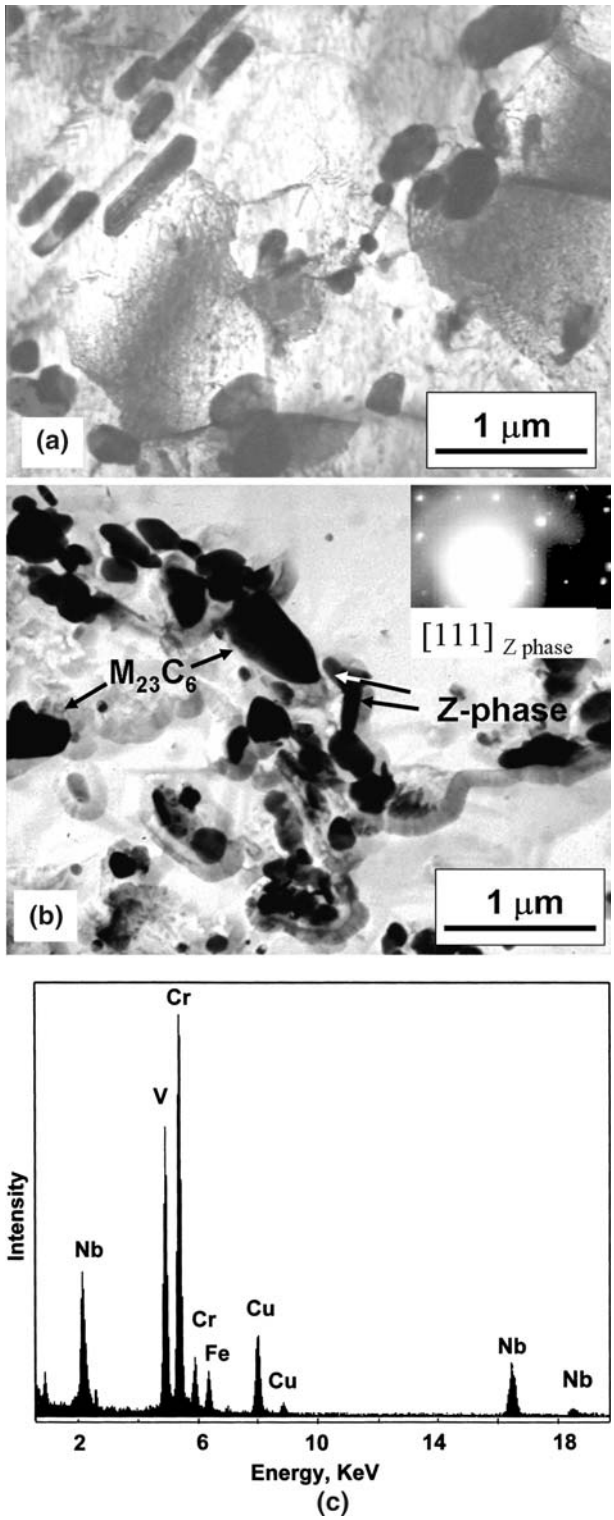

Fig. 19—TEM micrographs of intercritical HAZ of 9Cr-1MoVNb steel joint (creep tested at 923 K, 40 MPa, and t_r = 15,721 h): (*a*) thin foil, (*b*) extracted replica, and (*c*) EDXS, showing the presence of *Z* phase. (Copper peaks are from copper grid used to hold the specimen).

E. *Type-IV Cracking Resistance Steel*

Type-IV cracking in the fusion-welded components of power-generating utilities made out of the ferritic steels is reported as a grave concern.[5,6] Development of high-temperature creep-resistance ferritic steels is mostly based on the creep-rupture strength of the base metal giving less consideration to the joint strength.[26] The following measures could be adopted to develop higher type-IV cracking resistance steels.

(1) Increasing the solid-solution hardening of the steel on alloying with Mo, W, and Re,[27] while minimizing the precipitation of laves phase, which takes away the solute from the solution, is expected to increase the type-IV cracking resistance, as the strengthening is not expected to change appreciably on intercritical heating of tempered ferritic steel. The addition of W in 9Cr steel has been reported to increase the type-IV cracking resistance.[28]
(2) Increasing the recovery resistance of the dislocation substructure on stabilizing the $M_{23}C_6$ particles against coarsening, the type-IV cracking resistance of steel can be increased. Microalloying the steel with boron is reported to suppress the type-IV cracking by increasing coarsening resistance of the

$M_{23}C_6$ precipitate on replacing some of its carbon with boron.[29,30] The added boron content is to be judiciously adjusted with the nitrogen content to avoid BN formation so that boron is available for the desired effect.[31] Similarly, the addition of tungsten is reported to retard the coarsening kinetic of $M_{23}C_6$ precipitates in the 9Cr-0.5Mo-1.8WVNb (P92) steel over that in the 9Cr-1MoVNb (P91) steel to increase the type IV cracking resistance of 9Cr-0.5Mo-1.8WVNb steel.[28,32]

(3) Ensuring the stability of intragranular precipitates against thermal and creep exposures in ferritic steel can increase the resistance against type-IV cracking by reducing the strength disparity among the constituents of weld joint. The precipitation of highly stable MX type of precipitates (as in the 9Cr-1MoVNb) over the relatively unstable Mo_2C precipitate (as in the 2.25Cr-1Mo) has increased the type-IV cracking resistance of steel (Figure 6). Boron addition in the Cr-Mo steel is also reported to increase the stability of MX type of precipitates.[30] A suitable adjustment of composition within the specification range (reduction in carbon, nitrogen, and niobium contents) is reported to suppress type-IV cracking by reducing the strength disparity among the weld-joint constituents in the 9Cr-1MoVNb steel.[33] The *Z*-phase precipitation in steel dissolves the MX type of carbonitrides.[22] Retarding the precipitation of *Z* phase can increase the type-IV cracking resistance in steel as the enhance precipitation of *Z* phase was observed in the HAZ (Figure 19). The propensity of the *Z*-phase formation in steel increases with the contents of chromium, niobium, vanadium, and nitrogen. The reported higher reduction in creep-rupture strength (compared to the base metal) of 12Cr steel weld joint than the 9Cr steel weld joint[34] is probably due to higher propensity of *Z*-phase formation in the intercritical HAZ in the 12Cr steel than that in the 9Cr steel.

IV. CONCLUSIONS

1. Weld joint of Cr-Mo steels suffered a reduction in creep-rupture strength compared to their respective base metal due to type-IV cracking.
2. Type-IV cracking was manifested as preferential accumulation of creep strain coupled with creep cavitation in the intercritical region of HAZ.
3. Percentage reductions in creep-rupture strength of the joint increased with creep-rupture life and test temperature.
4. Susceptibility to the type-IV cracking depended on the steels and the operating temperature. The low-chromium 2.25Cr-1Mo steel was more prone to type-IV cracking than high-chromium 9Cr-1Mo and 9Cr-1MoVNb steels at lower temperatures. At higher temperatures, 9Cr-1MoVNb was more susceptible than 2.25Cr-1Mo steel.
5. Susceptibility to type-IV cracking of the steels could be rationalized on the basis of precipitation-strengthening mechanisms operating in the steels and the vulnerability of strengthening mechanisms to change on thermal exposure during weld thermal cycle.

ACKNOWLEDGMENTS

The authors thank Dr. B. Raj, Director, Indira Gandhi Center for Atomic Research (Kalpakkam, India), for his keen interest in this work. The authors thank S. Goyal for help carrying out the finite element analysis. The authors also thank N.S. Thampi for experimental assistance in conducting creep tests.

REFERENCES

1. C.D. Lundin and P. Liu: *WRC Bull.*, 2002, vol. 475, pp. 29–135.
2. K. Laha, K.S. Chandravathi, K. Bhanu Sankara Rao, and S.L. Mannan: *Int. J. Pressure Vessels Piping*, 2000, vol. 77, pp. 761–69.
3. H.J. Shüller, L. Haigh, and A. Woitscheck: *Der Machinenschaden*, 1974, vol. 47, pp. 1–13.
4. C.J. Middleton, J.M. Brear, R. Munson, and R. Viswanathan: *Proc. Advances in Materials Technology for Fossil Power Plants*, R. Viswanathan, W.T. Braker, and J.D. Parker, eds., University of Wales, Swansea, 2001, pp. 69–78.
5. S.J. Brett: *Proc. Advances in Materials Technology for Fossil Power Plants*, R. Viswanathan, W.T. Braker, and J.D. Parker, eds., University of Wales, Swansea, 2001, pp. 343–51.
6. I.A. Shibli: *Engineering Issues in Turbine Machinery, Power Plant and Renewables*, Trinity College, Dublin, Ireland, A. Strang, R.D. Conroy, W.M. Banks, M. Blacker, J. Leggett, G.M. McColvin, S. Simpson, M. Smith, F. Starr, and R.W. Vantone, eds., The Institute of Materials, Minerals and Mining, London, 2003, pp. 261–79.
7. K. Laha, K.S. Chandravathi, K. Bhanu Sankara Rao, and S.L. Mannan: *Heat Resistant Materials*, Gatlinburg, TN, 1995, pp. 399–404.
8. K.S. Chandravathi, K. Laha, K. Bhanu Sankara Rao, and S.L. Mannan: *Mater. Sci. Technol.*, 2001, vol. 17, pp. 559–65.
9. C.D. Lundin, J.A. Henning, R. Menon, and K.K. Khan: ORNL Report No. ORNL/Sub/81-07685/02&77, Oak Ridge National Laboratory, Oak Ridge, TN, 1987.
10. M. Nakashoro, S. Kihara, F. Kishimoto, and T. Fujimori: *ISIJ Int.*, 1990, vol. 30, pp. 823–28.
11. V.S. Srinivasan, K. Laha, K. Bhanu Sankara Rao, S.L. Mannan, and B. Raj: *Trans. Ind. Inst. Met.*, 2005, vol. 58 (2–3), pp. 255–59.
12. K. Laha, K.S. Chandravathi, P. Parameswaran, and S.L. Mannan: *Metall. Mater. Trans. A*, 2007, vol. 38A, pp. 58–68.
13. L. Dejun, K. Shinozaki, H. Kuriki, H. Harada, and K. Ohishi: *Sci. Technol. Weld. Join.*, 2003, vol. 8 (4), pp. 296–302.
14. G. Eggeler, A. Ramteke, M. Coleman, B. Chew, G. Peter, A. Burblies, J. Hald, C. Jefferey, J. Rantala, M. deWhite, and R. Mohrmann: *Int. J. Pressure Vessels Piping*, 1994, vol. 60, pp. 237–57.
15. B.G. Ivarsson and R. Sandstrom: in *Creep and Fracture of Engineering Materials and Structure*, B. Wilshire and D.R.J. Owen, eds., Pineridge Press, Swansea, 1981, pp. 661–69.
16. B.J. Cane: *Acta Metall.*, 1981, vol. 29, pp. 1581–91.
17. J.M. Vitek and R.H. Klueh: *Metall. Trans. A*, 1983, vol. 14A, pp. 1047–55.
18. P.J. Ennis, A. Zielinska-Lipiec, O. Wachter, and A. Czyrska-Filemonowicz: *Acta Mater.*, 1997, vol. 45 (12), pp. 4901–07.
19. R.G. Baker and J. Nutting: *J. Iron Steel Inst.*, 1956, vol. 192, pp. 257–68.
20. B.W. Jones, C.R. Hills, and D.H. Polonis: *Metall. Trans. A*, 1991, vol. 22A, pp. 1049–58.
21. K. Kimura, H. Kushima, F. Abe, K. Suzuki, S. Kumai, and A. Satoh: *Advanced Materials for 21st Century Turbines and Power Plant*, Cambridge, UK, 2000, A. Straang, W.M. Banks, R.D. Conroy, G.M. McColvin, J.C. Neal, and S. Simpson, eds., The Institute of Materials, London, 2000, pp. 590–602.

22. H.K. Danielsen and J. Hald: *Energy Mater.*, 2006, vol. 1 (1), pp. 49–57.
23. P.J. Ennis and A. Czyrska-Filemonowicz: *Sadhana*, 2003, vol. 28, Parts 3&4, pp. 709–30.
24. P. Roy and T. Lauritzen: *Weld. J.– Res. Suppl.*, 1986, pp. 45s–47s.
25. Y. Tsuchida, K. Okamoto, and Y. Tokunaga: *Weld. Int.*, 1996, vol. 10 (6), pp. 27–33.
26. F. Abe, M. Igarashi, S. Anikawa, M. Tabuchi, T. Itagaki, K. Kimura, and K. Yamaguchi: *Advanced Materials for 21st Century Turbines and Power Plant*, Cambridge, UK, 2000, A. Straang, W.M. Banks, R.D. Conroy, G.M. McColvin, J.C. Neal, and S. Simpson, eds., The Institute of Materials, London, 2000, pp. 129–42.
27. M. Morinaga, R. Hashizume and Y. Murata: *Materials for Advanced Power Engineering, Part 1*, Liege, Belgium, D. Coutsouradis, J.H. Davidson, J. Ewald, P. Greenfield, T. Khan, M. Malik, D.B. Meadowcroft, V. Regis, R.B. Scarlin, F. Schubert, and D.V. Thronton eds., Dordrecht, Kluwer Acedamic Publishers, 1994, pp. 319–28.
28. Y. Hasegawa, M. Ohgahi, and Y. Okamura: *Int. Conf. Advances in Materials Technology for Fossil Power Plants*, University of Wales, Swansea, April 5–6, 2001, R. Viswanathan, W.T. Braker, and J.D. Parker, eds., The Institute of Metals, London, 2001, pp. 457–66.
29. F. Abe, M. Tabuchi, M. Kondo, and S. Tsukamoto: *IJVP*, 2007, vol. 84, pp. 44–52.
30. P. Hofer, M.K. Miller, S.S. Babu, S.A. David, and H. Cerjak: *ISIJ Int.*, 2002, vol. 42, pp. S62–S66.
31. M. Tabuchi, H. Hongo, and Y. Takahashi: *Proc. ASME Pressure Vessels and Piping Division Conference*, Part III, Vancouver, BC, Canada, July 2006, pp. 23–27.
32. K. Sawada, M. Takeda, M. Maruyama, R. Ishii, M. Yamada, Y. Nagae, and R. Komine: *Mater. Sci. Eng.*, 1999, vol. A267, pp. 19–25.
33. N. Abe, Y. Kunisada, T. Sugiyama, and T. Nagamine: *Rivita Italian Delta Saldatura*, 1990, vol. 2, pp. 44–51.
34. M. DeWitte and C. Coussement: *Mater. High Temp.*, 1991, vol. 9 (4), pp. 178–84.